Electron–acoustic-phonon energy-loss rate in multicomponent electron systems with symmetric and asymmetric coupling constants

M. Prunnila*
VTT Micro and Nanoelectronics, P.O. Box 1000, FI-02044 VTT Espoo, Finland
(Received 17 November 2006; revised manuscript received 25 January 2007; published 25 April 2007)

We consider electron-phonon (*e-ph*) energy-loss rate in three-dimensional and two-dimensional multicomponent electron systems in semiconductors. We allow general asymmetry in the *e-ph* coupling constants (matrix elements), i.e., we allow the coupling to depend on the electron subsystem index. We derive a multicomponent *e-ph* power-loss formula, which takes into account the asymmetric coupling and links the total *e-ph* energy-loss rate to the density response matrix of the total electron system. We write the density response matrix within mean-field approximation, which leads to coexistence of symmetric energy-loss rate $F_S(T)$ and asymmetric energy-loss rate $F_A(T)$ with total energy-loss rate $F(T)=F_S(T)+F_A(T)$ at temperature T. The symmetric component $F_S(T)$ is equivalent to the conventional single-subsystem energy-loss rate in the literature, and in the Bloch-Grüneisen limit, we reproduce a set of well-known power laws $F_S(T) \propto T^{n_S}$, where the prefactor and power n_S depend on electron system dimensionality and electron mean free path. For $F_A(T)$ we produce a different set of power laws $F_A(T) \propto T^{n_A}$. Screening strongly reduces the symmetric coupling, but the asymmetric coupling is unscreened, provided that the intersubsystem Coulomb interactions are strong. The lack of screening enhances $F_A(T)$ and the total energy-loss rate $F(T)$. Especially, in the strong screening limit, we find $F_A(T) \gg F_S(T)$. A canonical example of strongly asymmetric *e-ph* matrix elements is the deformation potential coupling in many-valley semiconductors.

DOI: 10.1103/PhysRevB.75.165322 PACS number(s): 72.10.Di, 73.63.Hs, 63.20.Kr, 44.90.+c

I. INTRODUCTION

Electron-lattice energy loss in various bulk and low-dimensional semiconductor systems has attained a great deal of interest during the last few decades.[1] One reason for the extensive studies of electron-phonon (*e-ph*) energy relaxation arises directly from device applications. Another driving force is that the energy relaxation is connected to the versatile physics of microscopic electron-phonon interaction. Furthermore, the total *e-ph* energy-loss rate can be probed in hot electron experiments, which serve as a test for electron-lattice interaction.

The *e-ph* energy loss is highly sensitive to various parameters of the coupled *e-ph* system. The most important parameter is, of course, the nature of the electron-phonon interaction. In single-valley semiconductors, the electron-phonon interaction can be typically described by deformation potential (DP) or piezoelectric coupling constants.[2] In quantum wells also, other types of coupling due to heterointerface[3] or electric-field[4] induced quantum confinement may be important. In the above-mentioned electron lattice coupling mechanisms, the dependence of the *e-ph* matrix elements on the electronic variables, such as momentum, can be typically ignored. The situation is different, e.g., in metals where momentum dependency must be included due to the high Fermi level.[5] However, by simply setting the *e-ph* matrix elements to a constant is not the whole story, even for DP coupling in semiconductors. In many-valley (MV) systems, where the conduction-band minimum consist of several equivalent valleys, certain strain components lift the valley degeneracy, which directly shows that the *e-ph* DP coupling depends on the valley indices.[2,6] It is well known that this leads to an important role of the valley degree of freedom in the elastic properties and ultrasonic attenuation of doped MV semiconductors.[7–9] However, it was not until recently that the effect of MV-DP coupling was investigated in the context of the *e-ph* energy relaxation as well.[10] This brings us to the topic of this work: we present a theoretical discussion on *e-ph* energy-loss rate in carrier systems that consist of different components (subsystems), which can have different *e-ph* coupling constants, i.e., different matrix elements. Here we follow a terminology where the coupling is referred to as asymmetric if the *e-ph* matrix elements of the subsystems are different, and if they are the same, the coupling is referred to as symmetric. A typical example of asymmetric *e-ph* matrix elements is the MV-DP coupling.

This paper describes the total steady-state *e-ph* energy-loss rate (or power loss) in semiconductors in the presence of symmetric and asymmetric *e-ph* couplings. We will assume that the lattice and charge carriers are in separate internal equilibrium. Within this so-called temperature model,[11,12] the total energy-loss rate can be quite generally described by a symmetric power-loss formula[1,11,13–15]

$$P = F(T_e) - F(T_{ph}), \tag{1}$$

where T_e and T_{ph} are the electron and phonon temperatures, respectively. The exact form of the energy-loss rate (function) $F(T)$ requires microscopic derivation, but it can be phenomenologically linked to the *e-ph* energy relaxation time $\tau_{e\text{-}ph}$. This time scale is roughly equivalent to the thermal RC time constant defined by $G_{e\text{-}ph}^{-1}C_e$, where $G_{e\text{-}ph}=\delta F(T)/\delta T$ is the macroscopic electron-phonon thermal conductivity and C_e is the electron heat capacity. At low temperatures, $\tau_{e\text{-}ph}^{-1} \propto T_e^p$ and $C_e \propto T_e$, which leads to the well-known power law $F(T) \propto T^n$ $(n=p+2)$. This temperature dependency has been experimentally verified in various electron and hole systems, which exhibit different prefactor and power n, by utilizing

low-temperature carrier heating techniques (see, e.g., Refs. 1, 10, and 15–21 and references therein).

A single carrier component is equivalent to symmetric *e-ph* coupling, which is typically the unquestioned assumption made in microscopic derivations of Eq. (1) and $\tau_{e\text{-}ph}^{-1}$. However, the existence of the asymmetric coupling can have a large effect, because it is typically unscreened due to intersubsystem Coulomb interactions. This is the case even if the total electron system would seem to be at the strong screening limit, where the screening wave vector κ is larger than thermal phonon wave vector $q_T=k_BT/\hbar v_s$ (v_s is the velocity of sound). In MV semiconductors, the dependence of the DP coupling on valley indices is a source of strong asymmetric coupling and, due to lack of screening, this enhances the *e-ph* energy relaxation.[9,10] In these systems, the carrier subsystems (valleys) have a full spatial overlap, but modern micro- and nanofabrication techniques enable also the realization of artificial bilayers where two two-dimensional (2D) electron gases (2DEGs) form spatially separated subsystems. Now if asymmetric coupling exists in closely spaced bilayers, the *e-ph* energy-loss rate can be similarly enhanced as in MV systems. Here we will touch *e-ph* energy-loss rate in both MV semiconductors and bilayer systems.

This paper is organized as follows: In Sec. II A we derive the multicomponent version of Eq. (1) by utilizing Kogan's approach,[11,12] which connects $F(T)$ to the electron density response function. We will allow the *e-ph* matrix elements to depend on the electron subsystem indices, which introduces the multicomponent nature. We will assume that phonons cannot couple the electron subsystems directly. For example, in many-valley systems such direct coupling is relevant only for high-energy phonons.[1,2] Then in Secs. II B and II C, we write the density response function (here a matrix describing the multicomponent electron system) within mean-field approximation, which eventually leads to the coexistence of a symmetric energy-loss rate $F_S(T)$ and an asymmetric energy-loss rate $F_A(T)$ with the total energy-loss rate $F(T)=F_A(T)+F_S(T)$. In Sec. III A, we discuss about the general aspects of $F_A(T)$ and, in Sec. III B, we derive several analytical results in the Bloch-Grüneisen limit. For $F_S(T)$ we reproduce a set of analytical results, which shows well-known dependency on the parameters of the electron system, such as dimensionality and electron mean free path l_e. For $F_A(T)$ we find a different set of results and show that if the asymmetric and symmetric couplings have similar magnitude, then $F_A(T)\gg F_S(T)$ (provided that κ exceeds q_T). In Sec. III B, we also view the role of $F_A(T)$ in experiments and, finally, we conclude and summarize in Sec. IV.

II. THEORY

A. Electron-phonon energy-loss rate

We assume that a phonon with momentum $\hbar\boldsymbol{q}$ and energy $\hbar\omega$ cannot directly couple the electron subsystems, in which case the *e-ph* interaction is described via matrix elements $\mathcal{M}_{\boldsymbol{q},l}$, where $l=1,2,\ldots,L$ refers to an electron subsystem and L is the total number of subsystems. However, we will allow disorder-induced elastic coupling of the subsystems. The electron-phonon interaction Hamiltonian is now given by

$$H_{e\text{-}ph}=\sum_{\boldsymbol{q}}\sum_{l}(\mathcal{M}_{\boldsymbol{q},l}\rho_{\boldsymbol{q},l}^{\dagger}b_{\boldsymbol{q}}+\mathcal{M}_{\boldsymbol{q},l}^{*}\rho_{\boldsymbol{q},l}b_{\boldsymbol{q}}^{\dagger}), \tag{2}$$

where $b_{\boldsymbol{q}}$ ($b_{\boldsymbol{q}}^{\dagger}$) is the phonon annihilation (creation) operator. The electron-density operator $\rho_{\boldsymbol{q},l}=\Sigma_{\boldsymbol{k}}c_{\boldsymbol{k}-\boldsymbol{q},l}^{\dagger}c_{\boldsymbol{k},l}$, where $c_{\boldsymbol{k},l}$ ($c_{\boldsymbol{k},l}^{\dagger}$) is the electron annihilation (creation) operator in subsystem l. Following Refs. 11 and 12, the *e-ph* interaction will be considered as a perturbation Hamiltonian that will cause transitions from initial state $|i,\{n_{\boldsymbol{q}}\}_i\rangle$ with energy $\mathcal{E}_i$ to final state $|f,\{n_{\boldsymbol{q}}\}_f\rangle$ with energy $\mathcal{E}_f$. In state $|e,\{n_{\boldsymbol{q}}\}_p\rangle$, index e refers to electronic states and $\{n_{\boldsymbol{q}}\}_p$ is a set of phonon occupation numbers. The transition rate from initial to final state W_{fi} is given by the golden rule formula

$$W_{fi}=\frac{2\pi}{\hbar}|\langle f,\{n_{\boldsymbol{q}}\}_f|H_{e\text{-}ph}|i,\{n_{\boldsymbol{q}}\}_i\rangle|^2\delta(\mathcal{E}_i-\mathcal{E}_f). \tag{3}$$

By substituting Eq. (2) into Eq. (3), performing an ensemble average over the initial phonon and electronic states, and summing over final electronic states, we obtain the phonon emission and absorption rates as follows:

$$W_{em}(\boldsymbol{q})=\frac{2\pi}{\hbar}\sum_{i,f}\hat{w}_i\left|\left\langle f\left|\sum_{l}\mathcal{M}_{\boldsymbol{q},l}^{*}\rho_{\boldsymbol{q},l}\right|i\right\rangle\right|^2(N_{\boldsymbol{q}}+1)\delta(E_{i,f}-\hbar\omega), \tag{4a}$$

$$W_{ab}(\boldsymbol{q})=\frac{2\pi}{\hbar}\sum_{i,f}\hat{w}_i\left|\left\langle f\left|\sum_{l}\mathcal{M}_{\boldsymbol{q},l}\rho_{-\boldsymbol{q},l}\right|i\right\rangle\right|^2N_{\boldsymbol{q}}\delta(E_{i,f}+\hbar\omega). \tag{4b}$$

Here $\hat{w}_i$ is the weighting factor for the electron many-body state, the energy difference $E_{i,f}=E_i-E_f$, and $N_{\boldsymbol{q}}=\langle n_{\boldsymbol{q}}\rangle$. We assume that the phonon system can be described by a thermal distribution $N_{\boldsymbol{q}}=N_{T_{ph}}(\omega)=[\exp(\hbar\omega/k_BT_{ph})-1]^{-1}$ at temperature T_{ph} and by a well-defined phonon dispersion $\omega=\omega_{\boldsymbol{q}}$ (we ignore phonon renormalization and hot phonon effects[12]). The total *e-ph* energy-loss rate per d-dimensional electron volume V_e is given by the energy balance equation

$$\begin{aligned}P&=\frac{1}{V_e}\sum_{\boldsymbol{q}}\hbar\omega[W_{em}(\boldsymbol{q})-W_{ab}(\boldsymbol{q})]\\&=\frac{1}{V_e}\sum_{\boldsymbol{q}}\frac{\omega}{\hbar}[e^{-\hbar\omega/k_BT_e}-(1-e^{-\hbar\omega/k_BT_e})N_{\boldsymbol{q}}]\\&\quad\times\sum_{l,m}\mathcal{M}_{\boldsymbol{q},l}^{*}C_{l,m}(\boldsymbol{q},\omega)\mathcal{M}_{\boldsymbol{q},m},\end{aligned} \tag{5}$$

where the latter equality is obtained by utilizing $\hat{w}_f=\hat{w}_i\exp[(E_i-E_f)/k_BT_e]$ (T_e is the electron temperature). The correlator $C_{l,m}(\boldsymbol{q},\omega)$ in Eq. (5) is defined by

$$C_{l,m}(\boldsymbol{q},\omega)=2\pi\hbar\sum_{i,f}\hat{w}_f\langle f|\rho_{\boldsymbol{q},l}|i\rangle\langle i|\rho_{\boldsymbol{q},m}^{\dagger}|f\rangle\delta(E_{f,i}+\hbar\omega), \tag{6}$$

and it is connected to the density response matrix $\chi_{l,m}(\boldsymbol{q},\omega)$ through the standard fluctuation dissipation relation[22]

$$(1-e^{-\hbar\omega/k_BT_e})C_{l,m}(\boldsymbol{q},\omega) = -2\hbar V_e \,\mathrm{Im}\{\chi_{l,m}(\boldsymbol{q},\omega)\}. \quad (7)$$

Substituting Eq. (7) into Eq. (5) leads to microscopic definition of $F(T)$ in Eq. (1):

$$P = F(T_e) - F(T_{ph}), \quad (8a)$$

$$F(T) = \sum_{\boldsymbol{q}} \omega N_T(\omega) 2\boldsymbol{e}_{\boldsymbol{q}}^{\dagger}\hat{M}_{\boldsymbol{q}}^{\dagger}\,\mathrm{Im}\{-\hat{\chi}(\boldsymbol{q},\omega)\}\hat{M}_{\boldsymbol{q}}\boldsymbol{e}_{\boldsymbol{q}}. \quad (8b)$$

For the sake of clarity, we will denote matrices by a hat. Here the response matrix $\hat{\chi}_{l,m}(\boldsymbol{q},\omega)=\chi_{l,m}(\boldsymbol{q},\omega)$ depends on the properties of the electron system. Therefore, if the temperature dependency of $\hat{\chi}(\boldsymbol{q},\omega)$ is relevant, then $F(T)$ should be more generally written as $F(T,T_e)$, where T_e arises from the temperature dependency of $\hat{\chi}(\boldsymbol{q},\omega)=\hat{\chi}(\boldsymbol{q},\omega,T_e)$. We have introduced a useful matrix notation where the coupling matrix $\hat{M}_{\boldsymbol{q}}$ is related to the *e-ph* matrix element $\mathcal{M}_{\boldsymbol{q},l}$ through the relation

$$\mathcal{M}_{\boldsymbol{q},l} = \sum_{i=x,y,z} \{\hat{M}_{\boldsymbol{q}}\}_{l,i} e_i, \quad (9)$$

where e_i are components of the phonon polarization vector $\mathbf{e}_{\boldsymbol{q}}$ ($|\mathbf{e}_{\boldsymbol{q}}|=1$). If $M_{\boldsymbol{q},l}=M_{\boldsymbol{q},m}$ for all l,m or $L=1$, Eq. (8) reduces to the power-loss formula of Refs. 11, 12, and 15. (The equivalence with the expressions of Sergeev *et al.*[15] can be obtained by utilizing the mean-field response function given in Ref. 23.) The elastic intervalley scattering induced energy-loss rate derived in Ref. 10 is also a special case of Eq. (8).

The obtained power-loss formula applies to any type of *e-ph* coupling mechanism that does not depend on the electronic variables (momentum) in a single subsystem. However, here we will mainly limit our studies to deformation potential coupling to bulk acoustic phonons (in a volume V_{ph}), in which case the coupling matrix is given by

$$\hat{M}_{\boldsymbol{q}} = i\sqrt{\frac{\hbar}{2V_{ph}\rho\omega}}q\hat{\Xi}\hat{S}, \quad (10)$$

where ρ is the mass density of the crystal. We follow the notations of Ref. 10: the $L\times 6$ DP matrix $\hat{\Xi}$ contains the deformation potential coupling constants, and matrix $\hat{S}$ is the displacement-strain conversion matrix. The DP matrix depends on the properties of the electron system. The form of $\hat{S}$ follows from the relation $\epsilon_{\alpha\beta}=\frac{1}{2}(\partial u_\alpha/\partial\beta+\partial u_\beta/\partial\alpha)=iqu_{\boldsymbol{q}}(\tilde{q}_\beta e_\alpha+\tilde{q}_\alpha e_\beta)/2$, which couples the six symmetric strain components $\epsilon_{\alpha\beta}$ to components of displacement $\boldsymbol{u}$. With $\hat{S}$ this relation is simplified to $\epsilon_{\alpha\beta}=iqu_{\boldsymbol{q}}\Sigma_\gamma\hat{S}_{\alpha\beta,\gamma}e_\gamma$. By definition, $\hat{S}$ is a 6×3 matrix, which depends only on unit wave vector components, $\tilde{q}_\alpha=q_\alpha/q$, i.e., it depends on the direction of phonon propagation. In our notation, $\hat{M}_{\boldsymbol{q}}$ also contains the *e-ph* form factors. However, when deriving the analytical results (Sec. III B), we mainly set these form factors to unity, which is a reasonable approximation if we are far from the threshold $q_Tt=1$ (t is the thickness of the electron system).

B. Energy-loss rate with mean-field density response

Next, we assume that the electronic system can be described with the response of the noninteracting system $\hat{\chi}_0(\boldsymbol{q},\omega)$ under the external field plus the induced field of all electrons, i.e., we use the standard mean-field approach [random-phase approximation (RPA)].[24] The RPA density response and dielectric function, generalized to a multicomponent system, are given by

$$\hat{\chi}(\boldsymbol{q},\omega) = \hat{\chi}_0(\boldsymbol{q},\omega)\hat{\varepsilon}^{-1}(\boldsymbol{q},\omega), \quad (11a)$$

$$\hat{\varepsilon}(\boldsymbol{q},\omega) = \hat{1} - \hat{V}\hat{\chi}_0(\boldsymbol{q},\omega), \quad (11b)$$

where matrix $\hat{V}$ contains the interaction potentials. The elements $\hat{V}_{ij}=V_{ij}=V_d(\boldsymbol{q})F_d^{ij}(\boldsymbol{q})$, where $V_d(\boldsymbol{q})=e^2/4\varepsilon_0(2/q)^{d-1}$ is the d-dimensional ($d=2,3$) Fourier transform of the Coulomb interaction and $F_d^{ij}(\boldsymbol{q})$ are the Coulomb form factors (ε_0 is the background semiconductor dielectric constant). Here we will consider two cases: (1) the 2D and/or three-dimensional (3D) subsystems are fully overlapping (many-valley/band, MV) or (2) two 2DEG layers separated by distance z_0 (bilayer). These cases are covered with form factor $F_d^{ij}(\boldsymbol{q})=[\delta_{ij}+(1-\delta_{ij})\exp(-qz_0)]^{3-d}$ (if $1/q$ greatly exceeds the width of the individual layers in 2D).

To study the energy-loss rate of the electron system, we must invert the dielectric matrix, which is a formidable task for arbitrary L, $\hat{V}$, and $\hat{\chi}_0(\boldsymbol{q},\omega)$. For two subsystems ($L=2$), the inversion is tractable and well known from bilayer Coulomb drag effect (see, e.g., Ref. 25). Furthermore, it is easy to show that if $\hat{V}\hat{\chi}_0=\hat{A}+(1-b)\hat{1}$, where matrix $\hat{A}$ follows symmetry $\hat{A}_{ij}=\hat{A}_{kj}$ for all i, j, and k, then $\hat{\varepsilon}^{-1}(\boldsymbol{q},\omega)=b^{-1}[\hat{1}+\hat{A}/(b-\mathrm{Tr}(\hat{A}))]$. This form covers, e.g., the case where all interactions are similar and $\hat{\chi}_0(\boldsymbol{q},\omega)$ is arbitrary: $\hat{V}_{ij}=V(\boldsymbol{q})$, $\hat{A}=\hat{V}\hat{\chi}_0(\boldsymbol{q},\omega)$, and $b=1$. Here we will mainly concentrate on a transparent model where all intrasubsystem and all intersubsystem dynamics are similar, respectively. In this case we have $\{\hat{\chi}_0\}_{ij}=\chi_d\delta_{ij}+\chi_{od}(1-\delta_{ij})$. We further define $\chi_0=\chi_d+(L-1)\chi_{od}$ and $\chi_1=-L\chi_{od}$ when $\hat{\chi}_0(\boldsymbol{q},\omega)$ is given by

$$\hat{\chi}_0(\boldsymbol{q},\omega) = \chi_0(\boldsymbol{q},\omega)\hat{1} + \chi_1(\boldsymbol{q},\omega)\hat{Q}_A. \quad (12)$$

Here $\hat{Q}_A=\hat{1}-\hat{Q}_S$ with $\{\hat{Q}_S\}_{ij}=1/L$, and these matrices have a useful property $\hat{Q}_i\hat{Q}_j=\delta_{ij}\hat{Q}_i$. We can either use the properties of $\hat{Q}_i$ to invert the dielectric function or note that now we also have $\hat{V}\hat{\chi}_0=\hat{A}+b\hat{1}$. We find

$$\hat{\varepsilon}^{-1}(\boldsymbol{q},\omega) = \varepsilon_S^{-1}(\boldsymbol{q},\omega)\hat{Q}_S + \varepsilon_A^{-1}(\boldsymbol{q},\omega)\hat{Q}_A, \quad (13)$$

where the scalar dielectric functions are $\varepsilon_S(\boldsymbol{q},\omega)=1-[V_{11}+(L-1)V_{12}]\chi_0(\boldsymbol{q},\omega)$ and $\varepsilon_A(\boldsymbol{q},\omega)=1-(V_{11}-V_{12})[\chi_0(\boldsymbol{q},\omega)+\chi_1(\boldsymbol{q},\omega)]$. We can recognize that both of these have a similar form to the standard RPA dielectric function. They are actually well known from bilayer physics, and the poles of $\varepsilon_{S,A}^{-1}(\boldsymbol{q},\omega)$ are related to symmetric (optical) and asymmetric (acoustic) plasmons, respectively.[26,27]

Now by using Eqs. (11)–(13), we can divide $F(T)$ [Eq. (8b)] into symmetric (F_S) and asymmetric (F_A) terms:

$$F(T) = F_S(T) + F_A(T), \tag{14a}$$

$$F_i(T) = \sum_{\boldsymbol{q}} \omega_{\boldsymbol{q}} N_T(\omega) 2\,\mathrm{Im}\{-\chi_i\} \frac{M_i^2}{|\varepsilon_i(\boldsymbol{q},\omega)|^2}, \tag{14b}$$

$$M_i^2 = \boldsymbol{e}_{\boldsymbol{q}}^\dagger \hat{M}_{\boldsymbol{q}}^\dagger \hat{Q}_i \hat{M}_{\boldsymbol{q}} \boldsymbol{e}_{\boldsymbol{q}}, \tag{14c}$$

where $i=S,A$, $\chi_S=\chi_0(\boldsymbol{q},\omega)$, and $\chi_A=\chi_0(\boldsymbol{q},\omega)+\chi_1(\boldsymbol{q},\omega)$. We have introduced yet another notation: the effective matrix elements M_i^2, which are defined by quadratic forms and screened with the scalar dielectric functions $\varepsilon_i(\boldsymbol{q},\omega)$. The matrix elements compactly describe the contributions of symmetric (M_S^2) and asymmetric (M_A^2) *e-ph* couplings. Note that from the properties of $\hat{Q}_i$, it follows that the effective matrix elements obey $M_i^2 \geqslant 0$ and, therefore, also $F_i(T) \geqslant 0$.

If the *e-ph* interaction is mediated through DP coupling [Eq. (10)], then quadratic form $\Xi_i^2 = \boldsymbol{e}_{\boldsymbol{q}}^\dagger \hat{S}^\dagger \hat{\Xi}^\dagger \hat{Q}_{S,A} \hat{\Xi} \hat{S} \boldsymbol{e}_{\boldsymbol{q}}$ can be interpreted as a square of the deformation potential "constant." Note that Ξ_i is not a constant in the general case: it depends on the phonon polarization (arises from $\boldsymbol{e}_{\boldsymbol{q}}$) and direction of propagation (arises from $\hat{S}$). If the DP coupling is mediated by one isotropic dilatational coupling constant Ξ, which is the same for all subsystems, then we simply have $\Xi_i^2 = \Xi^2 |\boldsymbol{e}_{\boldsymbol{q}} \cdot \boldsymbol{q}/|\boldsymbol{q}||^2 \delta_{i,S}$.

C. Response function of noninteracting electrons

In order to perform quantitative analysis, we must know the response function of the noninteracting system $\hat{\chi}_0(\boldsymbol{q},\omega)$. In the pure limit $ql_e \gg 1$, the off-diagonal elements of $\hat{\chi}_0(\boldsymbol{q},\omega)$ are zero and, for the diagonal elements, we use the standard zero-kelvin expressions:[28,29]

$$\chi_0(\boldsymbol{q},\omega) = \begin{cases} -\nu \dfrac{k_F}{4q}[H(a_+) - H(a_-)], & \text{3D} \\ -\nu \dfrac{k_F}{q}\left[\dfrac{q}{k_F} + G(a_+,a_-)\right], & \text{2D} \end{cases} \tag{15a}$$

$$\simeq -\nu\left[1 + i\frac{\omega}{q v_F} K_d\left(a_+^2 - \frac{2\hbar\omega}{\varepsilon_F}\right)\right], \tag{15b}$$

where $a_\pm = \omega/q v_F \pm q/2k_F$, $H(x) = 2x + (x^2-1)\ln[(x-1)/(x+1)]$ [$\ln(z)$ branch: $|\mathrm{Im}\ln(z)| \leqslant \pi$], and $G(a_+,a_-) = -(a_+^2-1)^{1/2} + [2\theta(|a_-|-1)\theta(-a_-)-1](a_-^2-1)^{1/2}$. $\nu = \nu(\varepsilon_F)$ is the (dimensionality dependent) density of states at Fermi level $\varepsilon_F \gg k_B T$ and v_F is the Fermi velocity. Equation (15b) is small-$\boldsymbol{q}$ approximation, where $K_d(x) = (\pi/2)^{d-2}\theta(1-x)(1-x)^{(d-3)/2}$.

We include the effect of (static) disorder by introducing a phenomenological transport relaxation rate $\gamma = 1/\tau$, which is connected to Drude mobility by $\mu = e\tau/m$. We distinguish between intrasubsystem and intersubsystem scattering rates, which we denote by γ_0 and γ_1, respectively. The total scattering rate is given by $1/\tau = \gamma = \gamma_0 + (L-1)\gamma_1$. Now the components of Eq. (12) in the diffusive (hydrodynamic) limit $\omega\tau, ql_e \ll 1$, are given by the particle-number-conserving many-band response functions of Kragler and Thomas[30] (see also Ref. 9),

$$\chi_0(\boldsymbol{q},\omega) = -\nu \frac{iD_0 q^2}{\omega + iD_0 q^2}, \tag{16a}$$

$$\chi_1(\boldsymbol{q},\omega) = \chi_0(\boldsymbol{q},\omega)\frac{\omega}{iD_0 q^2}\frac{i\bar{\gamma}}{(\omega + i\bar{\gamma}) + iD_0 q^2}, \tag{16b}$$

where $D_0 = \frac{1}{d} v_F^2 \tau = \frac{1}{d} v_F l_e$ is the diffusion constant and $\bar{\gamma} = \frac{L}{2}\gamma_1$ is the total elastic intervalley and/or interband intersscattering rate. Note that $\chi_0(\boldsymbol{q},\omega)$ has the familiar diffusion pole form,[23] while the interband term $\chi_1(\boldsymbol{q},\omega)$ exhibits also a relaxation pole which is slightly shifted toward finite q. The absorptive part of $\chi_A = \chi_0(\boldsymbol{q},\omega) + \chi_1(\boldsymbol{q},\omega)$, which enters $F_A(T)$, is

$$\mathrm{Im}\,\chi_A = -\frac{\nu(\bar{\gamma} + D_0 q^2)\omega}{(\bar{\gamma} + D_0 q^2)^2 + \omega^2}. \tag{17}$$

This simply states that in the diffusive limit there are two competing time scales which determine the energy relaxation: intervalley scattering time $1/\bar{\gamma}$ and diffusion time $1/D_0 q^2$ over the length scale $1/q$.

III. DISCUSSION AND ANALYTICAL RESULTS

A. General aspects

As $F_i(T) \geqslant 0$ holds always, the symmetric and asymmetric energy-loss rates in Eq. (14) provide separate additive energy relaxation channels. The appearance of two clearly distinguishable energy relaxation terms (channels) F_S and F_A follows from our symmetric choice of the response $\hat{\chi}_0(\boldsymbol{q},\omega)$ [Eq. (12)]. If we would relax the symmetry of $\hat{\chi}_0(\boldsymbol{q},\omega)$, more complicated cross terms with variable signs would also appear. However, here we will concentrate on the symmetric response, which captures the essential physics. The sufficient condition for finite asymmetric energy-loss rate F_A is that asymmetric coupling M_A differs from zero. The magnitude of F_A depends on diagonal and off-diagonal elements of $\hat{\chi}_0(\boldsymbol{q},\omega)$ through $\chi_A = \chi_0 + \chi_1 = \chi_d - \chi_{od}$. Therefore, $F_A > 0$ even if there is no direct coupling between the subsystems, i.e., even if $\chi_{od} = 0$ ($\chi_1 = 0$). This follows from an internal (dynamic) image charge effect which is due to Coulomb interaction between the subsystems.

The internal image charge effect is schematically depicted in Fig. 1 and it quantitatively follows from the properties of matrices $\hat{Q}_i$ in the inverse dielectric function of Eq. (13): let us assume that L is even and that the external field couples to the electron system through (scalar potential) $\boldsymbol{v}^{\mathrm{ext}}(\boldsymbol{q},\omega)$ with the components $\{\boldsymbol{v}^{ext}\}_l = v_l^{ext} = v^{ext,S} + v^{ext,A}(-1)^l$ (in Fig. 1, $v^{ext,S} = v^{ext,A}$). Here v_l^{ext} describes the (phonon) field interaction potential to subsystem l. Now the effective potential felt by the full electron system is $\boldsymbol{v}^{eff} = \hat{\varepsilon}^{-1}(\boldsymbol{q},\omega)\boldsymbol{v}^{ext}$, where $v_l^{\mathrm{eff}} = \varepsilon_S^{-1}(\boldsymbol{q},\omega)v^{ext,S} + \varepsilon_A^{-1}(\boldsymbol{q},\omega)v^{ext,A}$. Note that full asymmetry of $\boldsymbol{v}^{\mathrm{ext}}$ is, of course, not required. It is enough that $v_l^{ext} = v \neq v_m^{ext} = v + \delta v$ for one fixed $m \neq l$, and $\hat{Q}_A$ picks this particular component.

If the interaction between the subsystems is strong [$(V_{11} - V_{12})$ is small], then $\varepsilon_A(\boldsymbol{q},\omega) \sim 1$ and this quenches the

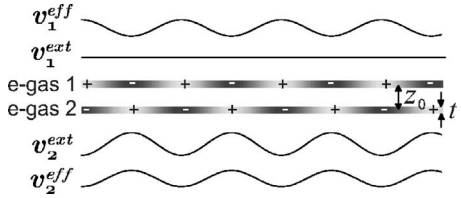

FIG. 1. Schematic cross section of a two-component system and illustration of the destruction of screening under an asymmetrically coupling field. The electron gases have thickness t and they are separated by a distance z_0. Note that $z_0>0$ describes a bilayer, whereas $z_0=0$ describes a many-valley system, which requires separation in reciprocal space. The solid curves describe the external (v_l^{ext}) and effective (v_l^{ext}) scalar coupling potentials in the plane of electron gas $l=1,2$. The $\pm$ signs describe the charge buildup due to the external (and effective) field in the two electron gases. See Sec. III A for further details.

screening of asymmetric coupling constants and enhances the total electron coupling to the external field. Thus, the effect described in this paper is most important in the strong screening limit, where the thermal phonon wavelength $2\pi/q_T$ exceeds the electron system screening length $2\pi/\kappa$. In this case, we expect that $F_S(T)\ll F_A(T)$ if $\varepsilon_A(\boldsymbol{q}_T,\omega_T)\sim 1$ ($\omega_T=k_BT/\hbar$) and $M_A^2\sim M_S^2$. Note that the asymmetric coupling also plays a role in medium screening systems $q_T\sim\kappa$ when $F_S(T)\sim F_A(T)$. On the other hand, the assumption $M_A^2\sim M_S^2$ may not always hold. It holds if asymmetric and symmetric couplings are directly mediated by DP interaction like in many-valley semiconductors or bilayer systems with different DP coupling constants. But the existence of nonzero M_A^2 may be due to the vibration of heterointerfaces[3] or *e-ph* form factors, which may give $M_S^2\gg M_A^2$. Then if $\varepsilon_S(\boldsymbol{q}_T,\omega_T)\gg\varepsilon_A(\boldsymbol{q}_T,\omega_T)$ still holds, we may have $F_A(T)\sim F_S(T)$ and both symmetric and asymmetric terms contribute to the total energy flow rate. We will inspect few different cases where either $F_S(T)\ll F_A(T)$ or $F_A(T)\sim F_S(T)$, in detail below.

B. Analytical studies of different systems

Table I shows asymptotic low-temperature expressions of Eq. (14) deep below the Bloch-Grüneisen limit $q_T=2k_F$ for different systems. Note that $F_S(T)$ is calculated assuming strong screening, but in many cases $F_A(T)$ is simply the weak/zero screening limit of $F_S(T)$ (see the discussion above). Before going into further details, we will briefly describe the general guidelines how the formulas in Table I are obtained and how they should be interpreted. First of all, the sum over $\boldsymbol{q}$ in Eq. (14b) is converted into a integral, and linear phonon dispersion relations $\omega=\omega_{\boldsymbol{q}}=v_sq$ are assumed. The sound velocity v_s refers to both transversal and longitudinal modes of the crystal and, therefore, all expressions must be summed over these modes (if coupling to both type of modes exists). Here we mainly concentrate on DP coupling and use the compact notation $\Xi_{S,A}^2=\boldsymbol{e}_{\boldsymbol{q}}^\dagger\hat{S}^\dagger\hat{\Xi}^\dagger\hat{Q}_{S,A}\hat{\Xi}\hat{S}\boldsymbol{e}_{\boldsymbol{q}}$ for the DP coupling constants [as discussed below Eq. (14)]. In the pure limit, $q_Tl_e\gg 1$, the formulas for $F_{S,A}(T)$ are obtained by utilizing Eq. (15b). In the diffusive limit, $q_Tl_e\ll 1$, they are obtained by utilizing Eqs. (16). For 2D electron system, vector $\boldsymbol{q}$ in $\hat{\chi}(\boldsymbol{q},\omega)$ refers to the parallel component $\boldsymbol{q}_\parallel=\boldsymbol{q}\sin\theta$, i.e., in 2D we set $\hat{\chi}(\boldsymbol{q},\omega)\to\hat{\chi}(\boldsymbol{q}_\parallel,\omega)$ (θ is the angle between $\boldsymbol{q}$ and the normal of the 2D electrons). The dimensionality also affects the Coulomb interaction [as described below Eq. (11a)] and is eventually seen in the screening wave vector $\kappa=2[e^2L\nu/4\varepsilon_0]^{1/(d-1)}$. Note that in the 2D diffusive limit, the F_A with $\ln(q_T)$ factors are derived with isotropic DP $\Xi_A^2=\Xi_0^2$. For arbitrary Ξ_A^2 analytical expressions cannot be found.[31]

We have divided the results in Table I into four categories: 3D pure, 2D pure, 3D diffusive, and 2D diffusive. These are described with common $F_S(T)$. The symmetric component $F_S(T)$ is equivalent to the conventional single-subsystem energy-loss rate in the literature. Indeed, if we assume coupling only to longitudinal phonons all symmetric energy-loss rates $F_S(T)$ agree with the expressions given in Refs. 1, 11, 14, and 15 and references therein. Note, however, that for the 2D diffusive case we have to set $1/\kappa l_s=0$ in order to find an equivalent expression to the $F_S(T)$ of Sergeev *et al.*[15] This small discrepancy follows from the approximation scheme of Ref. 15, which ignores dynamical effects in $\varepsilon_S(\boldsymbol{q},\omega_{\boldsymbol{q}})$. The importance of the dynamical effects in the diffusive $\chi_0(\boldsymbol{q},\omega)$ are determined by the threshold $\omega/D_0q^2=1$ or equivalently by $q_Tl_s=1$, which introduces the length scale $l_s=l_ev_F/v_sd$. However, the imaginary part of 2D RPA response is proportional to $\sin^2\theta/[1+l_s^2\sin^2\theta(q\sin\theta+\kappa)^2]$ and, therefore, in the strong screening limit, it is actually the parameter κl_s which is important and not q_Tl_s. This reasoning obviously applies also for the 3D case. Thus, both 3D and 2D diffusive limits $F_S(T)$ in Table I are valid if $\kappa l_s,\kappa/q_T\gg 1$.

Let us next inspect the asymmetric part of $F(T)$. We first focus on MV systems that are fully overlapping ($z_0=0$). First, notice that in pure cases the ratio $F_A/F_S=(\kappa/q_T)^m$, where $m=4$ (2) in 3D (2D). Thus, if screening is strong, $F_A\gg F_S$, as we would intuitively expect. In the diffusive limit, there are two competing internal relaxation mechanisms in the electron system, elastic intervalley scattering and diffusion, as already discussed below Eq. (17). When diffusion dominates over intervalley scattering, $\sqrt{\gamma/\bar{\gamma}}q_Tl_e\gg 1$ and, in the opposite situation, $\sqrt{\gamma/\bar{\gamma}}q_Tl_e\ll 1$. In contrast to $F_S(T)$, now the magnitude of q_Tl_s strongly affects the results. Note that actually all F_A in MV systems depend only very weakly on dimensionality and, when intervalley scattering dominates ($\sqrt{\gamma/\bar{\gamma}}q_Tl_e,k_BT/\hbar\bar{\gamma}\ll 1$), the 3D and 2D rates are similar, because then either screening or diffusion plays no role. Despite the finite mean free path and intervalley scattering rate, still $F_A\gg F_S$ holds in Table I. Recently, experiments on n^+ Si films were performed[10] in the range where the energy relaxation should be described by intervalley scattering induced *e-ph* energy-loss rate: the fourth and ninth F_A (from top) in Table I which have $F_A(T)\propto\frac{v_F}{\bar{\gamma}}\langle\Xi_A^2\rangle q_T^6\propto T^6$. This special case for $F_A(T)$ is also derived in Ref. 10, but by using a phenomenological approach which utilizes "classical" phonon attenuation rate. The experimental $F(T)$ for the n^+ Si samples coincide with the data of Table I and the ultrasonic attenuation data of Ref. 8.[32]

In 2D bilayer systems, the finite layer separation z_0 results in $\varepsilon_A(\boldsymbol{q},\omega)\neq 1$. If z_0 is small ($q_Tz_0\ll 1$), then $\varepsilon_A(\boldsymbol{q},\omega)\approx 1$

TABLE I. Symmetric $F_S(T)$ and asymmetric $F_A(T)$ contributions of energy-loss rate of Eqs. (14). The pure and diffusive categories are defined by $q_T l_e \gg 1$ and $q_T l_e \ll 1$, respectively. The Limits column gives additional assumptions used in calculating F_A. $z_0=0$ refers to many-valley systems and $z_0>0$ refers to bilayers. Temperature dependency comes from thermal phonon wave vector $q_T=k_BT/\hbar v_s$. The length scale $l_s=l_e v_F/v_s d$, the DP constants $\Xi_i^2=\boldsymbol{e}_{\boldsymbol{q}}^\dagger \hat{S}^\dagger \hat{\Xi}^\dagger \hat{Q}_i \hat{\Xi} \hat{S} \boldsymbol{e}_{\boldsymbol{q}}$, and the dielectric function $\varepsilon_A=1+\kappa z_0/2$. The bracket $\langle \cdots \rangle$ stands for average over solid angle. The F_A with $\ln(q_T)$ factors are derived using isotropic $\Xi_A^2=\Xi_0^2$. Both $F_{S,A}(T) \propto q_T^n$ are normalized with $(\hbar \nu v_s/2\pi^2 \rho v_F) B_{n-1}$, where $B_{n-1}=\Gamma(n)\zeta(n)=\int dx\, x^{n-1}/[\exp(x)-1]$. See Sec. III B for further details.

Category	$F_S(T)$	$F_A(T)$	F_A/F_S	Limits	$z_0=0$	$z_0>0$
3D pure	$\frac{\pi}{2\kappa^4}\langle \Xi_S^2 \rangle q_T^9$	$\frac{\pi}{2}\langle \Xi_A^2 \rangle q_T^5$	$\left(\frac{\kappa}{q_T}\right)^4$	–	×	
3D diffusive	$\frac{3}{l_e \kappa^4}\langle \Xi_S^2 \rangle q_T^8$	$\frac{3}{l_e}\langle \Xi_A^2 \rangle q_T^4$ $\frac{v_F}{v_S} l_s \langle \Xi_A^2 \rangle q_T^6$ $\frac{v_F}{\bar{\gamma}}\langle \Xi_A^2 \rangle q_T^6$	$\left(\frac{\kappa}{q_T}\right)^4$ $\left(\frac{\kappa^2 l_s}{q_T}\right)^2$ $\frac{\gamma}{\bar{\gamma}}\left(\frac{\kappa^2 l_e}{q_T}\right)^2$	$\sqrt{\frac{\gamma}{\bar{\gamma}}} q_T l_e, q_T l_s \gg 1$ $\sqrt{\frac{\gamma}{\bar{\gamma}}} q_T l_e, (q_T l_s)^{-1} \gg 1$ $\sqrt{\frac{\gamma}{\bar{\gamma}}} q_T l_e, k_B T/\hbar\bar{\gamma} \ll 1$	×	
2D pure	$\frac{1}{\kappa^2}\langle \sin\theta \Xi_S^2 \rangle q_T^7$	$\left\langle \frac{\Xi_A^2}{\sin\theta} \right\rangle q_T^5$ $\frac{(z_0)^2}{4\varepsilon_A^2}\left\langle \frac{\cos^2\theta \Xi_S^2}{\sin\theta} \right\rangle q_T^7$	$\left(\frac{\kappa}{q_T}\right)^2$ $\frac{(\kappa z_0)^2}{\varepsilon_A^2}$	– –	× 	 ×
2D diffusive	$\frac{2}{l_e \kappa^2}\left\langle \frac{\sin^2\theta \Xi_S^2}{(l_s\kappa)^{-2}+\sin^2\theta} \right\rangle q_T^6$	$\frac{1}{l_e}\Xi_0^2 q_T^4 \ln(q_T l_s)$ $\frac{v_F}{v_S} l_s \langle \sin^2\theta \Xi_A^2 \rangle q_T^6$ $\frac{v_F}{\bar{\gamma}}\langle \Xi_A^2 \rangle q_T^6$ $\frac{z_0^2}{8\varepsilon_A^2 l_e}\Xi_0^2 q_T^6 \ln(\varepsilon_A l_s q_T)$ $\frac{v_F l_s z_0^2}{4 v_S}\langle \sin^2\theta \cos^2\theta \Xi_S^2 \rangle q_T^8$	$\left(\frac{\kappa}{q_T}\right)^2$ $(\kappa l_s)^2$ $\frac{\gamma}{\bar{\gamma}}(\kappa l_e)^2$ $\frac{(\kappa z_0)^2}{\varepsilon_A^2}$ $(\kappa l_s z_0 q_T)^2$	$\sqrt{\frac{\gamma}{\bar{\gamma}}} q_T l_e, q_T l_s \gg 1$ $\sqrt{\frac{\gamma}{\bar{\gamma}}} q_T l_e, (q_T l_s)^{-1} \gg 1$ $\sqrt{\frac{\gamma}{\bar{\gamma}}} q_T l_e, k_B T/\hbar\bar{\gamma} \ll 1$ $(\varepsilon_A q_T l_s) \gg 1$ $(\varepsilon_A q_T l_s)^{-1} \gg 1$	× × × 	 × ×

$+\kappa z_0/2$ $(=\varepsilon_A)$. So far, we have assumed unity *e-ph* form factors, but now we partially relax this assumption and allow phase factors, which arise from finite z_0, in the *e-ph* coupling matrix. The finite layer separation introduces $\exp[\pm i q_z z_0/2] \approx 1 \pm i q_z z_0/2$ factor in the first $(+)$ and second $(-)$ lines of the DP matrix $\hat{\Xi}$, which gives rise to asymmetric coupling. It is easy to show that now $\hat{\Xi}^\dagger \hat{Q}_A \hat{\Xi} = \frac{1}{4} q_z^2 z_0^2 \hat{\Xi}^\dagger \hat{Q}_S \hat{\Xi}$, which leads to the bilayer $(z_0>0)$ F_A in Table I. For bilayers, where the asymmetric coupling is induced by phonon form factors, the ratio $F_A/F_S \sim 1$ and depends on the magnitude of the parameter κz_0.

If we would relax the symmetry of $\hat{\chi}_0(\boldsymbol{q},\omega)$ [Eq. (12)], then more complicated cross terms in addition to $F_{S,A}(T)$ would also appear in $F(T)$, as was already pointed out in Sec. III A. Especially, in bilayer systems, the study of such terms is an interesting and important problem of its own, but it will not be discussed in detail in this paper. Note, however, that if $(V_{11}-V_{12}) \approx 0 [\varepsilon_A(\boldsymbol{q},\omega) \approx 1]$ and $\hat{\chi}_0(\boldsymbol{q},\omega)$ is diagonal, then Eq. (14) approximately holds with $\mathrm{Im}\,\chi_{S,A} \simeq \mathrm{Im}\{\mathrm{Tr}[\hat{\chi}_0(\boldsymbol{q},\omega)]\}$ (provided that $\kappa > q_T$). In this case, the 2D F_A with $z_0=0$ in Table I qualitatively describes closely spaced bilayers with different DP coupling constants. One such system is the 2DEG bilayer realized in a double AlAs quantum well,[33,34] where the two electron gases are from conduction-band valleys with different symmetries (depending on sample parameters).[35] 2DEG bilayer systems can also be tuned between two-component and single-component systems by external gates. Note, however, that the gate electrode can affect and/or contribute to the *e-ph* relaxation processes if the gate-to-2DEG distance is small $(\lesssim q_T^{-1})$, because then the gate is simply one "component" of the total carrier system. This effect can be present in all gated samples, at least at sufficiently low temperatures.[36]

An interesting special case "bilayer" is a single quantum well with two populated subbands with energies E_0 and E_1. Phonons vibrate the heterointerfaces of the well (i.e., change spatially the quantum well width), which is a source of *e-ph*

coupling.[3] This coupling is defined by $\delta E_n \simeq 2E_n \partial u_z/\partial z$ and, if $E_1 - E_0 = \Delta E \gg k_B T$, it is a source of asymmetric coupling with $\Xi_A^2 = \tilde{q}_z^2 e_z^2 \Delta E$. Now we find (utilizing Table I), e.g., for a pure system $F_A \propto \Delta E^2 \left\langle \frac{\cos^2\theta |e_z|^2}{\sin\theta} \right\rangle q_T^5$ and $F_A/F_S \propto (\kappa/q_T)^2 (\Delta E/\Xi)^2$ (we have replaced Ξ_S with a dilatational DP constant Ξ). As typically $\Delta E/\Xi \ll 1$ applies, the role of asymmetric coupling in the case of interface vibration is important only if screening is very strong.

IV. SUMMARY AND CONCLUSIONS

We have discussed on general aspects of the energy-loss rate induced by symmetric and asymmetric *e-ph* couplings in 3D and 2D multicomponent electron systems. We derived multicomponent version of Kogan's power-loss formula [Eq. (8)], which takes into account the *e-ph* matrix element dependency on the electron subsystem indices and links the total *e-ph* energy-loss rate to the density response function (matrix) of the electron system. We adopted standard mean-field approximation to find the density response function. This led to coexistence of symmetric energy-loss rate $F_S(T)$ and asymmetric energy-loss rate $F_A(T)$ with total energy-loss rate $F(T) = F_S(T) + F_A(T)$ [Eq. (14)].

For $F_S(T)$ we reproduced a set of well-known low-temperature power laws $F_S(T) \propto T^{n_S}$, where the prefactor and power n_S depend, e.g., on electron system dimensionality and electron mean free path l_e. For $F_A(T)$ we derived a different set of power laws $F_A(T) \propto T^{n_A}$. Screening strongly reduces the symmetric coupling and, therefore, also $F_S(T)$. Whereas, the asymmetric coupling is typically unscreened, which enhances $F_A(T)$ and the total energy-loss rate $F(T)$. This enhancement is large if the asymmetric and symmetric coupling constants have similar magnitude, and screening is important. Under these assumptions $F_A(T) \gg F_S(T)$, which we quantitatively proved also for many special cases.

In many-valley semiconductors, the deformation potential coupling constants depend on valley indices, which are a source of strong asymmetric *e-ph* coupling. Our findings agree with recent hot electron experiments on doped many-valley semiconductor (n^+ Si). Furthermore, the effect described here should be present in various bilayer systems.

ACKNOWLEDGMENTS

This work has been partially funded by the Academy of Finland (Project No. 205467, CODE) and by the European Union (Contract No. 034236, SUBTLE). J. Ahopelto and J. M. Kivioja are acknowledged for useful discussions.

*Electronic address: mika.prunnila@vtt.fi

[1] B. K. Ridley, Rep. Prog. Phys. **54**, 169 (1991).
[2] J. Singh, *Physics of Semiconductors and Their Heterostructures* (McGraw-Hill, New York, 1993).
[3] F. T. Vasko and V. V. Mitin, Phys. Rev. B **52**, 1500 (1995).
[4] B. A. Glavin, V. A. Kochelap, T. L. Linnik, and K. W. Kim, Phys. Rev. B **71**, 081305(R) (2005).
[5] F. S. Khan and P. B. Allen, Phys. Rev. B **29**, 3341 (1984).
[6] C. Herring and E. Vogt, Phys. Rev. **101**, 944 (1956).
[7] R. W. Keyes, in *Solid State Physics: Advances in Research and Applications*, edited by F. Seitz and D. Turnbull (Academic, New York, 1967), Vol. 20, pp. 37–90.
[8] M. Dutoit, Phys. Rev. B **3**, 453 (1971).
[9] T. Sota and K. Suzuki, J. Phys. C **15**, 6991 (1982).
[10] M. Prunnila, P. Kivinen, A. Savin, P. Törmä, and J. Ahopelto, Phys. Rev. Lett. **95**, 206602 (2005).
[11] S. M. Kogan, Fiz. Tverd. Tela (Leningrad) **9**, 2474 (1962) [Sov. Phys. Solid State **4**, 1813 (1963)].
[12] S. Das Sarma, J. K. Jain, and R. Jalabert, Phys. Rev. B **41**, 3561 (1990).
[13] Y. Shinba, K. Nakamura, M. Fukuchi, and M. Sakata, J. Phys. Soc. Jpn. **51**, 157 (1982).
[14] P. J. Price, J. Appl. Phys. **53**, 6863 (1982).
[15] A. Sergeev, M. Y. Reizer, and V. Mitin, Phys. Rev. Lett. **94**, 136602 (2005).
[16] Y. Kawaguchi and S. Kawaji, Jpn. J. Appl. Phys., Part 2 **21**, L709 (1982).
[17] K. Hirakawa and H. Sakaki, Appl. Phys. Lett. **49**, 889 (1986).
[18] R. Fletcher, V. M. Pudalov, Y. Feng, M. Tsaousidou, and P. N. Butcher, Phys. Rev. B **56**, 12422 (1997).
[19] R. J. Zieve, D. E. Prober, and R. G. Wheeler, Phys. Rev. B **57**, 2443 (1998).
[20] R. Fletcher, Y. Feng, C. T. Foxon, and J. J. Harris, Phys. Rev. B **61**, 2028 (2000).
[21] X. P. A. Gao, G. S. Boebinger, A. P. Mills, A. P. Ramirez, L. N. Pfeiffer, and K. W. West, Phys. Rev. Lett. **94**, 086402 (2005).
[22] R. Kubo, Rep. Prog. Phys. **29**, 255 (1966).
[23] J. Rammer and H. Smith, Rev. Mod. Phys. **58**, 323 (1986).
[24] D. Pines and P. Nozieres, *The Theory of Quantum Liquids* (Benjamin, New York, 1966), Vol. I.
[25] A. G. Rojo, J. Phys.: Condens. Matter **11**, R31 (1999).
[26] S. Das Sarma and A. Madhukar, Phys. Rev. B **23**, 805 (1981).
[27] G. E. Santoro and G. F. Giuliani, Phys. Rev. B **37**, 937 (1988).
[28] J. Lindhard, K. Dan. Vidensk. Selsk. Mat. Fys. Medd. **28**, 1 (1954).
[29] F. Stern, Phys. Rev. Lett. **18**, 546 (1967).
[30] R. Kragler and H. Thomas, Z. Phys. B: Condens. Matter **39**, 99 (1980).
[31] The $\ln(q_T)$ terms in Table I result from the integral $I_{i,j}(x, \Xi_A^2) = \int_0^\infty dy\, y^i [\exp(y)-1]^{-1} \left\langle \frac{\sin^2\theta \cos^{2j}\theta \Xi_A^2}{(yx)^{-2}+\sin^4\theta} \right\rangle$, where $j=0$ ($j=1$) for $z_0 = 0$ ($z_0 > 0$). Excellent approximation for isotropic $\Xi_A^2 = \Xi_0^2$ and $x \gg 1$ is given by $I_{i,j}(x, \Xi_0^2) = \frac{1}{2}\Xi_0^2 \int_{y_0}^\infty dy\, y^i/[\exp(y)-1]^{-1}\{\ln(4yx-2) - j(2-1/yx)\}$, where y_0 is defined from condition $\{\cdots\}=0$. Eventually we find $I_{i,j}(x, \Xi_0^2) \approx \alpha_{i,j} \tilde{\Xi}_0^2 B_i \ln(x)$, where $\alpha_{i,j}$ is a constant of the order of unity.
[32] Note that τ_{iv} in Ref. 10 is related to $\bar{\gamma}$ through $\bar{\gamma} = 1/2\tau_{iv}$.
[33] K. Vakili, Y. P. Shkolnikov, E. Tutuc, E. P. De Poortere, and M.

Shayegan, Phys. Rev. Lett. **92**, 186404 (2004).
[34] M. Shayegan, E. D. Poortere, O. Gunawan, Y. Shkolnikov, E. Tutuc, and K. Vakili, cond-mat/0606158 (unpublished).
[35] In AlAs $F(T)$ also contains piezoelectric contributions, which are easy to calculate by adding the piezoelectric coupling to matrix $\hat{M}_q$.
[36] Note that the gate electron and 2DEG temperatures can be different, which can lead to photon cooling effects [D. R. Schmidt, R. J. Schoelkopf, and A. N. Cleland, Phys. Rev. Lett. **93**, 045901 (2004)].